Notes

Reactivity of the Cyanometalate Na[Cp'Mn(CO)₂CN] with Titanium, Zirconium, and Hafnium Halides. Crystal and Molecular Structure of the μ-Cyano μ-Oxo Tetranuclear Complex [Cp₂Zr{(μ-NC)MnCp'-(CO)₂}]₂(μ-O) (Cp = η-C₅H₅; Cp' = η-MeC₅H₄)

Pierre Braunstein,*,† Daniele Cauzzi,†,‡ David Kelly,†
Maurizio Lanfranchi,‡ and Antonio Tiripicchio‡

Laboratoire de Chimie de Coordination URA 416 CNRS,
Université Louis Pasteur, 4 rue Blaise Pascal,
F-67070 Strasbourg Cédex, France, and Istituto di Chimica
Generale ed Inorganica, Università di Parma, Centro di
Studio per la Strutturistica Diffrattometrica del CNR,
Viale delle Scienze, I-43100 Parma, Italy

### Introduction

In contrast to most carbonylmetalates of the transition metals, cyanide-substituted anionic complexes such as Na[Cp'Mn-(CO)₂CN] (Cp' = η-MeC₅H₄) do not exhibit a metal-centered HOMO. Instead, this orbital is essentially nitrogen-based, which favors coordination to metal centers through the cyanide moiety, thus generating Mn–CN–M' chain systems.[1] The cyanometalate ligand [Cp'Mn(CO)₂CN]⁻ has been observed to coordinate via the CN⁻ in both terminal and bridging modes.[2,3] More complex interactions can also be generated, notably in the octanuclear Pd₄Mn₄ cluster [(OC)Pd(μ-NC)MnCp'(CO)₂]₄, whose novel molecular architecture is characterized by an orthogonal arrangement of helical units.[3] This cluster was formed quantitatively by the reaction of [Cp'Mn(CO)₂CN]⁻ with [Pd₄(μ-CO)₄(μ-OAc)₄], and a diversity of palladium–cyanometalate interactions are generated which maintain the tetrameric Pd structure: a direct Mn–Pd bond and semibridging manganese-bound CO and CN ligands, as well as Mn–(μ-CN)–Pd bridges.

In order to further study the bonding capabilities of Na[Cp'Mn-(CO)₂CN], we have examined its reactivity with the titanocene, zirconocene, and hafnocene dichlorides, as well as with related titanium(III) and -(IV) precursors.

Results

Cp₂TiCl₂ (Cp = η-C₅H₅) reacts readily with 2 equiv of Na[Cp'Mn(CO)₂CN] to give the deep blue complex Cp₂Ti[(μ-NC)MnCp'(CO)₂]₂ (1) (eq 1). Characterization, including the observation of parent ions in the FAB mass spectrum, suggests 1 is monomeric with the intense color being derived from titanium–cyanometalate charge transfer. The corresponding zirconium and hafnium complexes, 2 and 3, are spectroscopically similar to 1. However, lacking in the same spectral region the charge-transfer interactions of 1, they appear paler. CpTiCl₃ and TiCl₄ also react with Na[Cp'Mn(CO)₂CN] to afford the deeply colored complexes 4 and 5, respectively. The former could be characterized as the disubstituted complex CpTi[(μ-NC)MnCp'-(CO)₂]₂Cl (eq 2). The relative inertness of the third chloride

$$Cp_2TiCl_2 \ + \ 2\,Na[Cp'Mn(CO)_2CN]$$

(1)
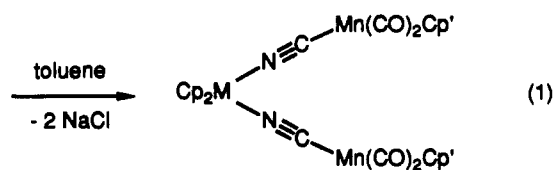
1 M = Ti deep blue (70%)
2 M = Zr red (75%)
3 M = Hf orange (65%)

(2)
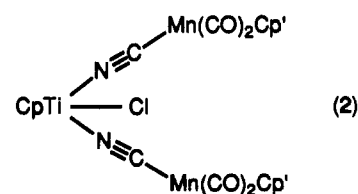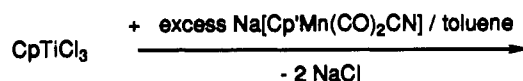
4 deep green (94%)

ligand toward substitution is surprising, although steric factors may be responsible. It is clear from the spectroscopic data obtained for 5 that chloride substitution has occurred. Since 5 is soluble in organic solvents, a formulation of the type found in the ionic complexes (NEt₄)₂[M{(μ-NC)Cr(CO)₅}₆] (M = Si, Ge) is unlikely.[4] However, the instability of the compound has prevented consistent or accurate elemental analysis, making an assessment of even the degree of chloride substitution impossible.

In fact, all the complexes 1–5 are air sensitive, undergoing hydrolysis before total decomposition. This is illustrated by the unexpected isolation of the μ-oxo complex [Cp₂Zr{(μ-NC)MnCp'-(CO)₂}]₂(μ-O) (6), in high yield during the attempted recrystallization of the chloro complex 2 from toluene/pentane. Traces of water reproducibly lead to transformation of 2 into 6. Under rigorously anhydrous conditions, 2 could only be obtained as a powder and no crystals were isolated. Since Na[Cp'Mn-(CO)₂CN] is protonated in the presence of acid,[5] a hydrolysis reaction of the form in Scheme I is likely. The corresponding titanium compound 7 was formed by the direct reaction of [Cp₂-TiCl]₂O with Na[Cp'Mn(CO)₂CN], although once again accurate elemental analysis proved impossible.

Facile titanium(IV) reduction was used to obtain the air-sensitive [Cp₂TiCl]₂, which on direct reaction with Na[Cp'Mn-(CO)₂CN] afforded the deep green titanium(IV) complex Cp₂Ti[(μ-NC)MnCp'(CO)₂]Cl (8) in 53% yield. The mechanism by which a redox reaction rather than simple chloride substitution occurs remains unclear. This complex was not observed during the slow addition of Na[Cp'Mn(CO)₂CN] to Cp₂TiCl₂ since the deep blue color associated with 1 was immediately observed (see

† Université Louis Pasteur.
‡ Università di Parma.
(1) Braunstein, P. In *Perspectives in Coordination Chemistry*; Williams A. F., Floriani, C., Merbach, A. E., Ed.; Verlag Helvetica Chimica Acta/VCH: CH-4010 Basel, Switzerland, 1992; pp 67–107.
(2) Oswald, B.; Powell, A. K.; Rashwan, F.; Heinze, J.; Vahrenkamp, H. *Chem. Ber.* 1990, *123*, 243.
(3) Braunstein, P.; Oswald, B.; Tiripicchio, A.; Tiripicchio Camellini, M. *Angew. Chem., Int. Ed. Engl.* 1990, *29*, 1140.

(4) Bär, E.; Fehlhammer, W. P.; Breitinger, D. K.; Mink, J. *Inorg. Chim. Acta* 1984, *82*, L17.
(5) Fischer, E. O.; Schneider, R. J. J. *J. Organomet. Chem.* 1968, *12*, P27.
(6) (a) Hamilton, D. M., Jr.; Willis, W. S.; Stucky, G. D. *J. Am. Chem. Soc.* 1981, *103*, 4255. (b) Merola, J. S.; Gentile, R. A.; Ansell, G. B.; Modrick, M. A.; Zentz, S. *Organometallics* 1982, *1*, 1731. (c) Dick, D. G.; Stephan, D. W. *Ibid.* 1990, *9*, 1910. (d) Matchett, S. A.; Norton, J. R.; Anderson, O. P. *Ibid.* 1988, *7*, 2228. (e) Schmid, G.; Stutte, B.; Boese, R. *Chem. Ber.* 1978, *111*, 1239. (f) Stutte, B.; Bätzel, V.; Boese, R.; Schmid, G. *Ibid.* 1978, *111*, 1603.
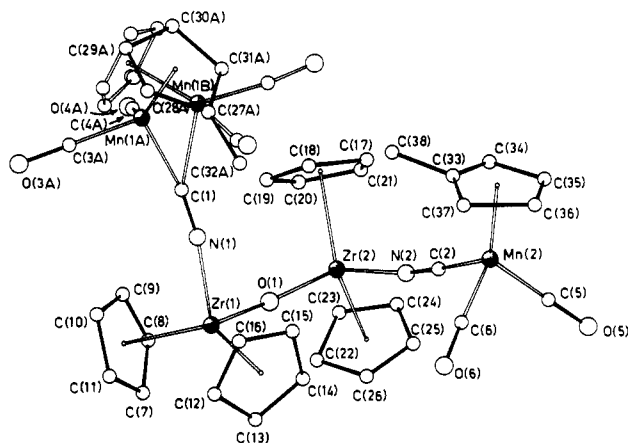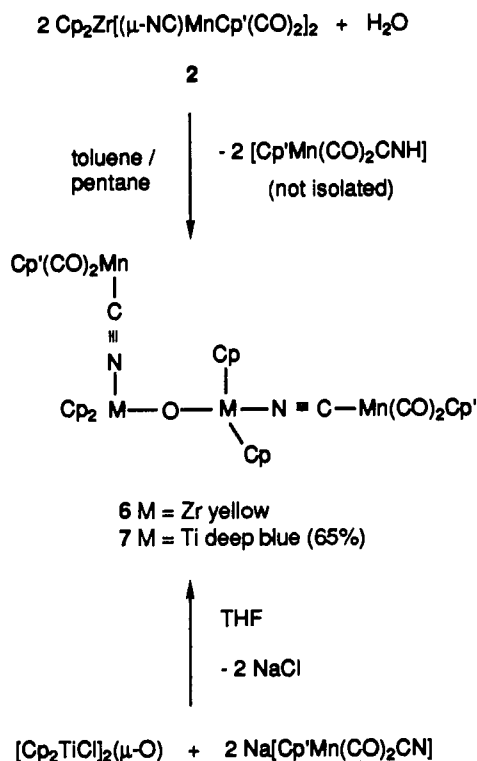
Figure 1. View of the structure of the complex [Cp$_2$Zr{(μ-NC)MnCp'-(CO)$_2$}]$_2$(μ-O) (6) with the atomic numbering scheme. One of the two MnCp'(CO)$_2$ groups [at Mn(1)] is disordered and distributed in two positions labeled as A and B. Only the numbering of the atoms in the position A is given for clarity.

Scheme I

2 Cp$_2$Zr[(μ-NC)MnCp'(CO)$_2$]$_2$ + H$_2$O

2

toluene /
pentane

− 2 [Cp'Mn(CO)$_2$CNH]

(not isolated)

6 M = Zr yellow
7 M = Ti deep blue (65%)

THF

− 2 NaCl

[Cp$_2$TiCl]$_2$(μ-O) + 2 Na[Cp'Mn(CO)$_2$CN]

above). Thus, the monosubstituted complex which must be an intermediate in the synthesis of 1 is very rapidly substituted by Na[Cp'Mn(CO)$_2$CN], suggesting it has a structure different from that of 8.

Description of the Crystal Structure of [Cp$_2$Zr{(μ-NC)MnCp'-(CO)$_2$}]$_2$O (6). The structure of 6 is shown in Figure 1 together with the atom-numbering scheme. Selected bond distances and angles are given in Table I. A cyanide ligand bridges the Mn and Zr metals of each Mn–CN–Zr unit, whereas an oxo bridge links the two Zr atoms. The oxo bridge is almost symmetrical [Zr-(1)–O(1) = 1.939(8) and Zr(2)–O(1) = 1.957(8) Å] and linear [Zr(1)–O–Zr(2) = 168.2(5)°], as generally observed for this system.[7] Although multiple bonding between the oxo ligand and the Zr(IV) centers is not required by the latter in order to achieve a 16e configuration, the relatively short Zr–O distances and the

(7) Reddy, K. P.; Petersen, J. L. *Organometallics* **1989**, 8, 2107 and references therein.

Table I. Selected Bond Distances (Å) and Angles (deg) for Complex 6[a]

Zr(1)–O(1)	1.939(8)	Zr(2)–O(1)	1.957(8)
Zr(1)–N(1)	2.15(1)	Zr(2)–N(2)	2.17(1)
Zr(1)–CE(1)	2.22(2)	Zr(2)–CE(3)	2.22(2)
Zr(1)–CE(2)	2.22(2)	Zr(2)–CE(4)	2.22(2)
Mn(1A)–C(1)	1.86(2)	Mn(1B)–C(1)	2.07(2)
Mn(1A)–C(3A)	1.72(3)	Mn(1B)–C(3B)	1.98(6)
Mn(1A)–C(4A)	1.83(3)	Mn(1B)–C(4B)	1.67(5)
Mn(1A)–CE(5A)	1.79(3)	Mn(1B)–CE(5B)	1.83(5)
Mn(2)–C(2)	1.86(2)	Mn(2)–CE(6)	1.80(2)
Mn(2)–C(5)	1.74(1)	Mn(2)–C(6)	1.73(2)
C(1)–N(1)	1.15(2)	C(2)–N(2)	1.17(2)
C(3A)–O(3A)	1.19(4)	C(4A)–O(4A)	1.08(4)
C(3B)–O(3B)	0.94(8)	C(4B)–O(4B)	1.18(7)
C(5)–O(5)	1.16(2)	C(6)–O(6)	1.18(3)
O(1)–Zr(1)–N(1)	97.9(4)	O(1)–Zr(2)–N(2)	98.1(4)
O(1)–Zr(1)–CE(1)	107.8(6)	O(1)–Zr(2)–CE(3)	107.6(6)
O(1)–Zr(1)–CE(2)	108.0(6)	O(1)–Zr(2)–CE(4)	109.1(8)
N(1)–Zr(1)–CE(1)	103.3(6)	N(2)–Zr(2)–CE(3)	104.2(7)
N(1)–Zr(1)–CE(2)	102.2(7)	N(2)–Zr(2)–CE(4)	102.7(9)
CE(1)–Zr(1)–CE(2)	132.1(9)	CE(3)–Zr(2)–CE(4)	130.1(10)
Zr(1)–N(1)–C(1)	167(1)	Zr(2)–N(2)–C(2)	170(1)
N(1)–C(1)–Mn(1A)	169(2)	Zr(1)–O(1)–Zr(2)	168.2(5)
N(1)–C(1)–Mn(1B)	152(2)	N(2)–C(2)–Mn(2)	177(1)
C(1)–Mn(1A)–C(3A)	99(1)	C(1)–Mn(1B)–C(3B)	88(2)
C(1)–Mn(1A)–C(4A)	88(1)	C(1)–Mn(1B)–C(4B)	109(2)
C(1)–Mn(1A)–CE(5A)	117(1)	C(1)–Mn(1B)–CE(5B)	102(2)
C(3A)–Mn(1A)–C(4A)	89(1)	C(3B)–Mn(1B)–C(4B)	84(2)
C(3A)–Mn(1A)–CE(5A)	125(1)	C(3B)–Mn(1B)–CE(5B)	136(2)
C(4A)–Mn(1A)–CE(5A)	130(1)	C(4B)–Mn(1B)–CE(5B)	130(2)
C(2)–Mn(2)–C(5)	94.3(7)	C(5)–Mn(2)–C(6)	92.5(8)
C(2)–Mn(2)–C(6)	92.0(8)	C(5)–Mn(2)–CE(6)	125.1(9)
C(2)–Mn(2)–CE(6)	118.9(8)	C(6)–Mn(2)–CE(6)	125.5(10)

[a] CE(1), CE(2), CE(3), and CE(4) are the centroids of the cyclopentadienyl rings, and CE(5A), CE(5B), and CE(6) are the centroids of the methylcyclopentadienyl rings.

linearity of the bridge could result from partial double-bond character arising from d$_\pi$–p$_\pi$ bonding between the filled p$_x$ and p$_y$ orbitals on O with empty d$_{xz}$ and d$_{yz}$ orbitals on Zr, as originally proposed by Dunitz and Orgel.[8] On the basis of orbital symmetry arguments previously discussed,[9] this bonding feature requires that the N(1)Zr(1)O(1)Zr(2)N(2) core must be nonplanar, with a dihedral angle between the two N–Zr–O planes near 90°. This is consistent with the situation in 6, where this dihedral angle is 98.6(3)°. This constraint is responsible for the skew character of the Mn–Zr–Zr–Mn arrangement. One of the two cyanides [C(2)–N(2)] is almost linearly bonded through the N and C atoms to the Mn and Zr atoms [C(2)–N(2)–Zr(2) = 170(1) and N(2)–C(2)–Mn(2) = 177(1)°]. The other cyanide [C(1)–N(1)], almost linearly linked to Zr(1) through the N(1) atom [C(1)–N(1)–Zr(1) = 167(1)°], is bonded through the C(1) atom of two disordered MnCp'(CO)$_2$ groups, distributed in two positions of different occupancy factors, 0.6 for Mn(1A) and 0.4 for Mn(1B), corresponding to an almost linear bonding with Mn(1A) [N(1)–C(1)–Mn(1A) = 169(2)°] and a bent arrangement with Mn(1B) [N(1)–C(1)–Mn(1B) = 152(2)°]. It is rather surprising that the two MnCp'(CO)$_2$ groups, with a Mn(1A)⋯Mn(1B) separation of 1.341(8) Å, are distributed in the two positions in a different ratio and that the structural analysis of another crystal of 6 gave the same results. Bent M–CN–M' arrays have been previously observed in cyanometalate complexes, and these results tend to indicate that there may not be a large energy difference between the linear and slightly bent arrangements, so that packing effects could play an important role. Packing effects are probably responsible for the disorder observed in the solid-state structure of 6.

All four metal atoms exhibit a tetrahedral coordination if one considers the centroids of the Cp and Cp' rings. The coordination

(8) (a) Dunitz, J. D.; Orgel, L. E. *J. Chem. Soc.* **1953**, 2594. (b) Lin, Z.; Hall, M. B. *Inorg. Chem.* **1991**, 30, 3817 and references therein.
(9) (a) Lauher, J. W.; Hoffmann, R. *J. Am. Chem. Soc.* **1976**, 98, 1729. (b) R. Petersen, J. L. *J. Organomet. Chem.* **1979**, 166, 179.

around the two Zr atoms involves two Cp ligands, the O atom, and a N atom from the cyanide ligand, whereas that around the Mn atoms involves one Cp' and three C atoms, two from carbonyl groups and one from the cyanide ligand. To our knowledge, this represents the first reported structure with a cyanide bridging between a zirconium atom and a transition metal. Two structures have been reported in which the Zr atoms are involved in an oxo bridge and in a bonding with a nitrogen atom: the centrosymmetric [{Me$_3$Si)$_2$N}$_2$ZrMe]$_2$O complex, with an imposed linear Zr–O–Zr bridge [Zr–O = 1.950(1) Å] and Zr–N bonds with bis-(trimethylsilyl)amino ligands of average value 2.081(1) Å,[10] and the anionic [Zr$_2$Cl$_3$O(C$_4$H$_4$N)$_2$(Cp*)$_2$]$^-$ complex, with an imposed C_2 symmetry [Zr–O = 1.910(6) Å and Zr–O–Zr = 132.5(8)°] and Zr–N bonds with pyrrolyl ligands of 2.21(1) Å.[11]

Discussion

It is interesting to relate the products obtained in these reactions between group 14 complexes and [Cp'Mn(CO)$_2$CN]$^-$ with those containing the 18e and isosteric metalate [CpMo(CO)$_3$]$^-$. Titanium(IV) and titanium(III) complexes have been characterized which contain the CpMo(CO)$_3$ fragment linked, not by a metal–metal bond, but via a μ-η^2 bridging carbonyl, as in Cp*$_2$-Ti(Me)(μ-OC)Mo(CO)$_2$Cp[6a] or in Cp$_2$Ti(THF)(μ-OC)Mo-(CO)$_2$Cp.[6b,c] Similarly, Cp'$_2$Zr(μ-OC)Mo(CO)$_2$Cp moieties have been characterized in zirconium(IV) complexes.[6d] The M(μ-OC)M' linkage also relieves steric hindrance about M, as exemplified by the structure of CpTi[Co(CO)$_4$][(μ-OC)-Co$_3$(CO)$_9$]$_2$,[6e] Cp$_2$Zr[(μ-OC)Co$_3$(CO)$_9$]$_2$, and Cp$_2$Hf[(μ-OC)-Co$_3$(CO)$_9$]$_2$,[6f] which contain the bulky tricobalt clusters as substituents. Whereas with soft metal centers, the [CpMo(CO)$_3$]$^-$ unit binds through the metal and the [Cp'Mn(CO)$_2$CN]$^-$ unit through the nitrogen (exceptionally also through the metal),[1-3] they behave more similarly toward Lewis acid centers, owing to their significant oxygen (Mo case) and nitrogen (Mn case) Lewis basicity.

Experimental Section

A. Reagents and Physical Measurements. All reactions were performed in Schlenk-type flasks under nitrogen. Solvents were purified and dried under nitrogen by conventional methods. Infrared spectra were performed in the 4000-400-cm^{-1} range on a Perkin-Elmer 398 spectrophotometer or Bruker IFS66 FT-IR, while UV spectra were recorded on a Shimdazu UV260 spectrophotometer. ^{1}H NMR spectra were recorded at 200.13 MHz on a FT Bruker WP-200SY instrument.

B. Syntheses. Na[Cp'Mn(CO)$_2$CN], [Cp$_2$TiCl]$_2$, and [Cp$_2$-TiCl]$_2$O were produced by published methods.[5,12,13] CpTiCl$_3$ and Cp$_2$MCl$_2$ (M = Ti, Zr, Hf) were obtained from Aldrich and used without further purification.

Cp$_2$Ti[(μ-NC)MnCp'(CO)$_2$]$_2$ (1). Cp$_2$TiCl$_2$ (0.200 g, 0.80 mmol) was dissolved in 50 mL of toluene, and Na[Cp'Mn(CO)$_2$-CN] (0.384 g, 1.60 mmol) was added against a flow of nitrogen. The resultant slurry was stirred for 4 h, during which an intensely deep blue solution developed. The solution was filtered and the solvent subsequently removed at reduced pressure to afford **1** as a deep blue solid. **1** was extracted with toluene (50 mL) and the solution filtered through *ca.* 10 cm of dry Celite. The solvent was again removed and the solid washed with pentane (2 × 20 mL) before being dried in vacuo (0.341 g, 70%): mp 116–118 °C; IR (C$_7$H$_8$)ν(CN) 2018 m, 2001 s, ν(CO) 1926 m, 1890 s cm^{-1}; (Nujol) ν(CN) 2027 m, 2017 m, 1999 s, ν(CO) 1934 m, 1920 m, 1875 s cm^{-1}; ^{1}H NMR (C$_7$D$_8$) δ 1.87 (s, 6 H, 2 C$_5$H$_4$CH_3), 4.34 (m, 8 H, 2 C$_5$H$_4$CH$_3$), 5.79 (s, 10 H, 2 Cp); UV–vis (C$_7$H$_8$) λ 709

(10) Planalp, R. P.; Andersen, R. A. *J. Am. Chem. Soc.* **1983**, *105*, 7774.
(11) Atwood, J. L.; Rogers, R. D.; Vann Bynum, R. *Acta Crystallogr., Sect. C* **1984**, *40*, 1812.
(12) Coutts, R. S. P.; Wailes, P. C.; Martin, R. L. *J. Organomet. Chem.* **1973**, *47*, 375.
(13) Chivers, T.; Ibrahim, E. D. *Can. J. Chem.* **1973**, *51*, 815.

(ϵ 7000), 390 (8600) nm; FAB$^+$ mass spectrum *m/z* 610.0 (20%, M), 554.0 (40%, M – 2CO), 546.0 (60%, M – C$_5$H$_4$), 490.0 (65%, M – 2CO – C$_5$H$_4$), 394.0 (40%, M – Cp'Mn(CO)$_2$CN). Anal. Calcd for C$_{28}$H$_{24}$Mn$_2$N$_2$O$_4$Ti (*M* = 610.3): C, 55.1; H, 3.9; N, 4.6. Found: C, 55.9; H, 4.4; N, 4.3.

Cp$_2$Zr[(μ-NC)MnCp'(CO)$_2$]$_2$ (2). **2** was prepared by the same route as **1** using Cp$_2$ZrCl$_2$ (0.100 g, 0.34 mmol) and Na[Cp'-Mn(CO)$_2$CN] (0.163 g, 0.68 mmol). **2** was isolated as a red solid (0.167 g, 75%): mp 120–122 °C; IR (C$_7$H$_8$) ν(CN) 2015 m, 1995 sh, ν(CO) 1920 m, 1880 s cm^{-1}; IR (Nujol) ν(CN) 2027 m, 2014 m, 1997 s, ν(CO) 1910 m, 1864 s cm^{-1}; ^{1}H NMR (C$_7$D$_8$) δ 2.02 (s, 6 H, 2 C$_5$H$_4$CH_3), 4.21 (m, 8 H, 2 C$_5$H$_4$CH$_3$), 5.90 (s, 10 H, 2 Cp); FAB$^+$ mass spectrum *m/z* 652 (20%, M), 596 (40%, M – 2CO), 588 (60%, M – C$_5$H$_4$), 532 (65%, M – 2CO – C$_5$H$_4$), 436 (40%, M – Cp'Mn(CO)$_2$CN). Anal. Calcd for C$_{28}$H$_{24}$-Mn$_2$N$_2$O$_4$Zr (*M* = 653.4): C, 51.4; H, 3.7; N, 4.3. Found: C, 50.6; H, 3.7; N, 4.3.

Cp$_2$Hf[(μ-NC)MnCp'(CO)$_2$]$_2$ (3). **3** was also prepared by a method analogous to that for **1** with Cp$_2$HfCl$_2$ (0.261 g, 0.69 mmol) and Na[Cp'Mn(CO)$_2$CN] (0.346 g, 1.44 mmol). **3** was isolated as an orange solid (0.330 g, 65%): mp 122–125 °C; IR (C$_7$H$_8$) ν(CN) 2020 m, 1995 s, ν(CO) 1918 m, 1878 s cm^{-1}; IR (Nujol) ν(CN) 2037 m, 2019 m, 2008 m, 1911 s, ν(CO) 1918 m, 1904 m, 1860 s, 1848 s cm^{-1}; ^{1}H NMR (C$_7$D$_8$) δ 1.91 (s, 6 H, 2 C$_5$H$_4$CH_3), 4.32 (m, 8 H, 2 C$_5$H$_4$CH$_3$), 5.94 (s, 10 H, 2 Cp); UV–vis (C$_7$H$_8$) 345 (ϵ 7600) nm; FAB$^+$ mass spectrum *m/z* 678.0 (30%, M – C$_5$H$_4$), 622.0 (100%, M – 2CO – C$_5$H$_4$), 528.0 (20%, M – Cp'Mn(CO)$_2$CN). Anal. Calcd for C$_{28}$H$_{24}$-HfMn$_2$N$_2$O$_4$ (*M* = 740.9): C, 45.4; H, 3.2; N, 3.8. Found: C, 45.2; H, 3.4; N, 3.2.

CpTi[(μ-NC)MnCp'(CO)$_2$]$_2$Cl (4). CpTiCl$_3$ (0.121 g, 0.55 mmol) and Na[Cp'Mn(CO)$_2$CN] (0.504 g, 2.11 mmol) were stirred in toluene (50 mL) for 1 h. The pale yellow CpTiCl$_3$ coloration rapidly gave way to an intense deep blue-green solution. After 1 h, the solution was filtered and the solvent evaporated to give **4** as a deep green solid (0.300 g, 94%): mp 150 °C dec; IR (C$_7$H$_8$) ν(CN) 2040 m, 1995 s, ν(CO) 1898 m, 1860 w cm^{-1}; ^{1}H NMR (C$_7$D$_8$) δ 1.90 (s, 6 H, 2 C$_5$H$_4$CH_3), 4.40 (m, 8 H, 2 C$_5$H$_4$CH$_3$), 6.67 (s, 5 H, Cp). Anal. Calcd for C$_{23}$H$_{14}$ClMnN$_2$O$_2$-Ti (*M* = 580.7): C, 47.6; H, 3.3; N, 4.0. Found: C, 47.3; H, 3.9; N, 3.9.

Complex 5. TiCl$_4$ (0.104 g, 0.56 mmol) and Na[Cp'Mn(CO)$_2$-CN] (0.550 g, 2.30 mmol) were stirred in toluene (50 mL) for 1 h. The pale yellow TiCl$_4$ coloration rapidly gave way to an intense deep blue-green solution. After 1 h, the solution was filtered and the solvent evaporated to give **5** as a deep blue solid (0.254 g): mp 80 °C dec; IR (C$_7$H$_8$) ν(CN) 2040 m, 1990 s, ν(CO) 1890 vs, 1850 sh cm^{-1}; IR (Nujol) ν(CN) 2015 m, 1990 s, ν(CO) 1935 m, 1890 s, 1840 m cm^{-1}; ^{1}H NMR (C$_7$D$_8$) δ 1.60 (s, 3 H, C$_5$H$_4$CH_3), 4.10 (m, 4 H, C$_5$H$_4$CH$_3$); FAB$^+$ mass spectrum *m/z* 640.0 (10%, Ti{(μ-NC)MnCp'(CO)$_2$}$_3$ – 2CO), 512.0 (15%, Ti{(μ-NC)MnCp'(CO)$_2$}$_3$ – 2CO – 2C$_5$H$_4$), 456.0 (20%, Ti{(μ-NC)MnCp'(CO)$_2$}$_3$ – 2CO – 2C$_5$H$_4$).

[Cp$_2$Zr{(μ-NC)MnCp'(CO)$_2$}]$_2$O (6). Yellow crystals of this complex were obtained during the recrystallization of **2** from toluene/pentane: IR (KBr) ν(CN) 2026 m, 2016 sh, ν(CO) 1923 sh, 1910 s, 1868 s, 1854 s cm^{-1}; ^{1}H NMR (C$_7$D$_8$) δ 1.97 (s, 6 H, 2 C$_5$H$_4$CH_3), 4.44 (m, 8 H, 2 C$_5$H$_4$CH$_3$), 6.28 (s, 20 H, 4 Cp). Anal. Calcd for C$_{38}$H$_{34}$Mn$_2$N$_2$O$_5$Zr$_2$ (*M* = 891.0): C, 51.2; H, 3.9; N, 3.1. Found: C, 52.0; H, 3.9; N, 3.1.

[Cp$_2$Ti{(μ-NC)MnCp'(CO)$_2$}]$_2$O (7). [Cp$_2$TiCl]$_2$O was prepared by the air oxidation of [Cp$_2$TiCl]$_2$ and recrystallized from CH$_2$Cl$_2$/Et$_2$O.[13] [Cp$_2$TiCl]$_2$O (0.380 g, 0.86 mmol) was slurried in THF solution with Na[Cp'Mn(CO)$_2$CN] (0.422 g, 1.77 mmol) to immediately afford an intensely deep blue solution and a brown slurry. Filtration and removal of the solvent in vacuo afforded **7** as a deep blue solid (0.487 g, 65%) (*M* = 806.4): mp 138–141 °C; IR (C$_7$H$_8$) ν(CN) 2032 m, ν(CO) 1911 m, 1859 s cm^{-1}; ^{1}H

Table II. Crystallographic Data for Complex **6**

mol formula	$C_{38}H_{34}Mn_2N_2O_5Zr_2$
mol wt	891.01
cryst syst	monoclinic
space group	$P2_1/c$
radiation (λ, Å)	graphite-monochr Mo Kα (0.710 73)
a, Å	11.182(3)
b, Å	12.081(3)
c, Å	27.013(5)
β, deg	96.58(2)
V, Å^3	3625(1)
Z	4
D_{calcd}, g cm^{-3}	1.632
F(000)	1784
crystal dimens, mm	0.13 × 0.21 × 0.25
linear abs, cm^{-1}	12.47
$R(F_o)^a$	0.0507
$R_w(F_o)^b$	0.0684

$^a R = \sum ||F_o| - |F_c||/\sum |F_o|$. $^b R_w = [\sum (|F_o| - |F_c|)^2/\sum w(F_o)^2]^{1/2}$.

NMR (C$_7$D$_8$) δ 1.62 (s, 6 H, 2 C$_5$H$_4$C*H*$_3$), 4.35 (m, 8 H, 2 C$_5$*H*$_4$-CH$_3$), 5.85 (s, 20 H, 4 Cp).

Cp$_2$Ti{(μ-NC)MnCp'(CO)$_2$}Cl (8). A THF solution of [Cp$_2$-TiCl]$_2$ was prepared in situ by the aluminum foil reduction of Cp$_2$TiCl$_2$ (0.300 g, 1.21 mmol).[12] The resultant green THF solution was directly filtered onto Na[Cp'Mn(CO)$_2$CN] (0.290 g, 1.21 mmol) to immediately afford an intensely deep green solution. THF was removed in vacuo and the solid extracted with toluene (50 mL). Filtration of a large quantity of insoluble material and removal of the toluene solvent afforded **8** as a deep green solid (0.274 g, 53%): mp 128 °C; IR (C$_7$H$_8$) ν(CN) 2025 m, 2016 s, ν(CO) 1914 m, 1885 s cm^{-1}; IR (Nujol) ν(CN) 1995 s, ν(CO) 1810 m, 1860 s cm^{-1}; ^{1}H NMR (C$_7$D$_8$) δ 1.87 (s, 3 H, C$_5$H$_4$C*H*$_3$), 4.33 (m, 4 H, C$_5$*H*$_4$CH$_3$), 5.80 (s, 5 H, Cp), 5.87 (s, 5 H, Cp). Anal. Calcd for C$_{19}$H$_{17}$ClMnNO$_2$Ti (*M* = 429.7): C, 53.1; H, 4.3; N, 3.3. Found: C, 53.2; H, 4.3; N, 3.1.

C. X-ray Crystal Structure Determination of [Cp$_2$Zr{(μ-NC)-MnCp'(CO)$_2$}]$_2$O (6). A crystal of **6**, of approximate dimensions 0.13 × 0.21 × 0.25 mm, was used for the X-ray analysis. The crystallographic data are summarized in Table II. Data were collected at room temperature on a PW 1100 Philips single-crystal diffractometer using the graphite-monochromated Mo Kα radiation and the $\theta/2\theta$ scan mode. All reflections with θ in the range 3–24° were measured; of 5711 independent reflections, 2151, having $I > 2\sigma(I)$, were considered observed and used in the analysis. The individual profiles have been analyzed according to Lehmann and Larsen.[14] The intensity of one standard reflection was measured after 50 reflections as a general check on crystal and instrument stability; no significant change in the measured intensities was observed during the data collection. No correction for the absorption effect was applied. Only the observed reflections were used in the structure solution and refinement.

The structure was solved by Patterson and Fourier methods. One of the two MnCp'(CO)$_2$ groups, namely that bound to the nonlinear bridging cyanide, was found disordered and distributed in two positions of 0.6 and 0.4 occupancy factors, respectively. The difficult separation of the two images of the disordered groups accounts for the relatively inaccurate results obtained in the structure determination. It is interesting to note that the results obtained from the X-ray analysis of a different crystal were quite similar (same disorder and same inequivalent distribution of the two moieties). The refinement was carried out by full-matrix least squares first with isotropic and then with anisotropic thermal parameters in the last cycles for all the non-hydrogen atoms excepting those of the disordered ligands around Mn(1) and the Cp' carbon atoms around Mn(2). The final cycles of refinement were carried out on the basis of 412 variables. After the last cycles, no parameter shifted by more than 0.74 esd. The largest remaining peak in the final difference map was equivalent to

(14) Lehmann, M. S.; Larsen, F. K. *Acta Crystallogr., Sect. A* **1974**, *30*, 580.

Table III. Atomic Coordinates (×10^4) and Equivalent Isotropic Thermal Parameters (Å^2 × 10^4), with ESD's in Parentheses for the Non-Hydrogen Atoms of the Complex **6**

atom	*x/a*	*y/b*	*z/c*	*U*
Zr(1)	1142(1)	358(1)	1491(1)	596(5)^a
Zr(2)	367(1)	3243(1)	915(1)	618(5)^a
Mn(1A)	4929(3)	1521(3)	2587(2)	567(18)^a
Mn(1B)	5398(6)	1930(6)	2190(3)	726(30)^a
Mn(2)	3145(2)	2516(2)	–458(1)	802(10)^a
O(1)	598(7)	1791(7)	1232(3)	619(34)^a
O(3A)	4364(19)	–77(20)	3334(8)	1254(77)
O(4A)	3179(22)	3053(21)	2922(8)	1101(80)
O(3B)	6486(44)	520(44)	1513(18)	1414(177)
O(4B)	5495(33)	3724(37)	1516(14)	1536(141)
O(5)	1493(11)	3086(10)	–1328(5)	1101(56)^a
O(6)	2560(14)	174(11)	–564(5)	1286(71)^a
N(1)	2905(11)	852(13)	1821(5)	982(62)^a
N(2)	1351(11)	2939(10)	281(4)	792(54)^a
C(1)	3741(15)	1143(17)	2075(7)	1217(87)^a
C(2)	2032(14)	2753(12)	–9(5)	673(58)^a
C(3A)	4573(22)	594(23)	3031(9)	709(71)
C(4A)	3866(29)	2503(24)	2811(9)	757(78)
C(3B)	5948(51)	972(45)	1666(21)	825(150)
C(4B)	5451(40)	2927(41)	1764(19)	964(143)
C(5)	2146(14)	2856(14)	–978(5)	775(69)^a
C(6)	2787(16)	1126(21)	–509(6)	975(86)^a
C(7)	–665(18)	–315(24)	1865(6)	1021(92)^a
C(8)	–465(17)	768(21)	2052(7)	1015(94)^a
C(9)	595(19)	777(17)	2347(6)	877(82)^a
C(10)	1102(16)	–295(24)	2390(7)	1000(86)^a
C(11)	320(23)	–987(17)	2086(9)	1059(98)^a
C(12)	1512(28)	–1492(15)	1103(6)	1049(98)^a
C(13)	518(15)	–957(21)	786(8)	1017(88)^a
C(14)	1013(20)	–36(15)	577(5)	847(81)^a
C(15)	2257(23)	–19(21)	749(9)	1150(110)^a
C(16)	2506(21)	–876(27)	1063(8)	1155(113)^a
C(17)	2058(17)	4646(20)	1034(8)	910(84)^a
C(18)	2320(15)	3835(18)	1403(10)	929(86)^a
C(19)	1452(27)	3867(21)	1734(8)	1197(112)^a
C(20)	657(21)	4701(22)	1574(9)	1151(102)^a
C(21)	1023(24)	5191(14)	1140(9)	1158(102)^a
C(22)	–1791(15)	2722(32)	857(13)	1268(122)^a
C(23)	–1719(17)	3933(34)	915(10)	1184(118)^a
C(24)	–1389(21)	4323(22)	491(15)	1247(127)^a
C(25)	–1238(19)	3438(38)	170(10)	1387(137)^a
C(26)	–1485(20)	2511(25)	382(13)	1181(115)^a
C(27A)	6138(20)	1235(19)	1995(9)	512(61)
C(28A)	6672(25)	803(24)	2489(11)	911(88)
C(29A)	6832(34)	1495(36)	2834(14)	886(129)
C(30A)	6478(27)	2665(27)	2637(12)	841(87)
C(31A)	5944(38)	2491(34)	2124(15)	1106(134)
C(32A)	5916(61)	494(61)	1544(25)	1830(312)
C(27B)	4730(40)	2540(37)	2857(14)	768(119)
C(28B)	5897(46)	2947(37)	2797(17)	986(146)
C(29B)	6690(44)	1981(49)	2884(19)	777(165)
C(30B)	5973(63)	1065(51)	2905(22)	1473(204)
C(31B)	4965(49)	1473(49)	2915(22)	923(166)
C(32B)	3721(50)	3340(45)	2987(18)	935(170)
C(33)	4701(18)	2886(18)	46(8)	1133(63)
C(34)	4230(21)	3868(22)	–107(9)	1498(82)
C(35)	4375(19)	3813(19)	–614(8)	1312(69)
C(36)	4838(16)	2779(15)	–714(7)	1032(56)
C(37)	5060(24)	2013(23)	–211(10)	1801(102)
C(38)	4805(38)	2848(38)	594(18)	3381(221)

^{a} Equivalent isotropic *U* defined as one-third of the trace of the orthogonalized U_{ij} tensor.

about 0.6 e/Å^3. In the final cycles of refinement, a weighting scheme $w = K/[\sigma^2(F_o) + gF_o^2]$ was used; at convergence, the *K* and *g* values were 0.449 and 0.0076, respectively. The atomic scattering factors, corrected for the real and imaginary parts of anomalous dispersion, were taken from ref. 15.

All calculations were carried out on the CRAY X-MP/12 computer of the Centro di Calcolo Elettronico Interuniversitario

(15) *International Tables for X-Ray Crystallography*; Kynoch Press: Birmingham, England, 1974; Vol. IV.

dell'Italia Nord-Orientale (CINECA, Casalecchio Bologna) and on the GOULD POWERNODE 6040 of the Centro di Studio per la Strutturistica Diffrattometrica del CNR, Parma, using the SHELX-76 and SHELXS-86 systems of crystallographic computer programs.[16]

The final atomic coordinates for the non-hydrogen atoms are given in Table III.

(16) Sheldrick, G. M. SHELX-76: program for crystal structure determination, University of Cambridge, England, 1976. Sheldrick, G. M. SHELXS-86: program for the solution of crystal structure, University of Göttingen, 1986.

Supplementary Material Available: Anisotropic and isotropic thermal parameters for the non-hydrogen atoms (Table SI), complete bond distances and angles (Table SII), and crystallographic data (Table SIII) (5 pages). Ordering information is given on any current masthead page.